DOI: 10.1515/sspjce-2020-0007

Wind flow around buildings of basic shapes with and without a wind-adaptive envelope

Lenka Kabošová, Stanislav Kmeť, Dušan Katunský

Technical University of Košice, Slovakia
Faculty of Civil Engineering, Institute of Architectural Engineering
e-mail: lenka.kabosova@tuke.sk, stanislav.kmet@tuke.com, dusan.katunsky@tuke.sk

Abstract

Together with the natural environment, the built, artificial environment represents a barrier to the wind fluxes. Especially in the densely built cities, the wind flow pattern and the wind speed are considerably altered by buildings, which can lead to zones of an accelerated wind and turbulent flow. Incorporating the wind into the early conceptual stage of architectural design, this reciprocal interaction of the built environment and the wind fluxes can be analyzed and controlled to create zones of calmer wind around buildings. Presently, building envelopes are designed to withstand extreme load cases, which, however, demands thicker and bulkier structures. The subject of this study is a proposal and investigation of a lightweight, adaptive building envelope, which is able of a local, passive morphing in the wind. This local shape change leads to creating a textured, dimpled building surface; the final shape depends on the wind direction and force. The wind-induced dimpled surface influences the wind flow around the building, as well as surface wind pressure acting on the building, and the drag force. The analysis of three fundamental building shapes using the CFD (Computational Fluid Dynamics) simulation is performed for the variants with and without the proposed adaptive envelope. Concluding from the wind simulations, the wind flow can be decelerated, the turbulence reduced, and calmer zones around buildings can be created, by certain conditions. Moreover, the envelope, morphing with the instant wind force, can contribute to the reduction of the surface wind suction on buildings. Strikingly, the dimpled geometry of the wind-adaptive envelope can decrease the wind drag force by up to 28.4 %, which is again dependent on the global form, as well as the initial wind speed.

Key words: wind flow, adaptive building envelope, digital design, CFD analysis

1 Introduction

Designing architecture based on its performance in the wind was still a new approach in architectural practice not that long ago [1,2]. This method, however, slowly penetrates the architectural, as well as the civil engineering area [3]. Continuously advancing digital design and analysis tools contribute to the smooth integration of wind analysis to the design process. In the early conceptual design stage, fast decision-making is crucial. When it comes to the evaluation of the building performance in the wind, CFD simulations can help in estimating the wind-architecture interactions, and subsequently, in developing wind-formed designs.

When designing for arid lands, for instance, the wind can be utilized to provide natural ventilation [4]. Porous building envelopes, for example, can contribute to the natural ventilation of tall buildings and thus protect them from the heat load, as well as manage exhaust air [5]. Moreover, pollutant dispersion can be predicted by employing CFD simulations [6,7]. In the zones with the turbulent, cold and strong wind, both local and global building forms, together with the urban configuration of buildings, can influence the reduction of the unfavorable wind effects [8]. The small scale elements, creating a bumpy surface, can contribute to affecting the overall building aerodynamics [9].

1.1 Computational tools in the early design stage

Designing for the fluctuating wind conditions in the external environment, incorporating available computational tools in the early conceptual design stage leads to improving the performance of the design under the existing wind conditions [7,8,9] compared to evaluating the wind performance of the completed project in the later design stages, which is less effective, and the subsequent wind optimization of the design much costlier [9]. Among architects, Rhinoceros, as well as its algorithmic designing plug-in Grasshopper, are well-known 3D modeling software. Controlling the design parametrically according to the results of the design's performance in the wind, a wind-adaptive urban, architectural, or structural design can be created as a result of an iterative process. Creating more design alternatives varying in form, relative rotation, and scale means more options to choose from in the given wind conditions. The wind-driven form-finding using CFD (Computational Fluid Dynamics) analysis leads to the wind-based optimization of the intended design, which can retroactively control or modify the wind speed and flow pattern [10,11]. CFD simulations can either run through a stand-alone program or be integrated into a 3D software (e.g., Rhinoceros). If the design and the wind analysis can be completed in one working environment, the wind optimization is much more fluid, which speeds up the iterative process of finding the most suitable design option in the specific wind situation. When employing the simulations in the design process, a question might arise, whether the virtual simulation results are comparable with reality, and the physical wind tunnel experiments. Older studies [6,15], as well as new research, has already tested and validated the accuracy of CFD simulations compared to the wind tunnel measurements or field measurements [8,9,12,13]. The results obtained from modern CFD tools are in good agreement with wind tunnel experiments. This study proposes to engage the simulations in the early design phase for obtaining an idea of the interactions of the wind with the built environment. In the later design stages, after the best-performing designs are picked based on the CFD results, these can be then tested in the physical wind tunnel.

1.2 The Eurocode 1

The structural design of buildings exposed to the wind effects is coordinated by the Eurocode 1 EN 1991-1-4:2005. The guidelines are valid in most EU countries except Bulgaria, Croatia, and Romania. However, some of the non-EU countries, such as Iceland, Norway, as well as Switzerland, use Eurocode 1 to design building structures subjected to the wind. National annexes contain a country-specific wind map depicting the fundamental value of the basic wind velocity, v_{b0}. This value represents the characteristic 10-minute mean wind velocity,

irrespective of wind direction and season, at the height of 10 m above flat open country terrain with low vegetation. It is used for the structural design of buildings, as a maximum wind load that a structure has to withstand. The example of the Central and Mediterranean Europe wind map with values of v_{b0} is depicted in (Fig. 1) [18]. The value of 24 m/s (86.4 km/h), representing the fundamental value of the basic wind velocity for Slovakia is used in the wind analysis tests.

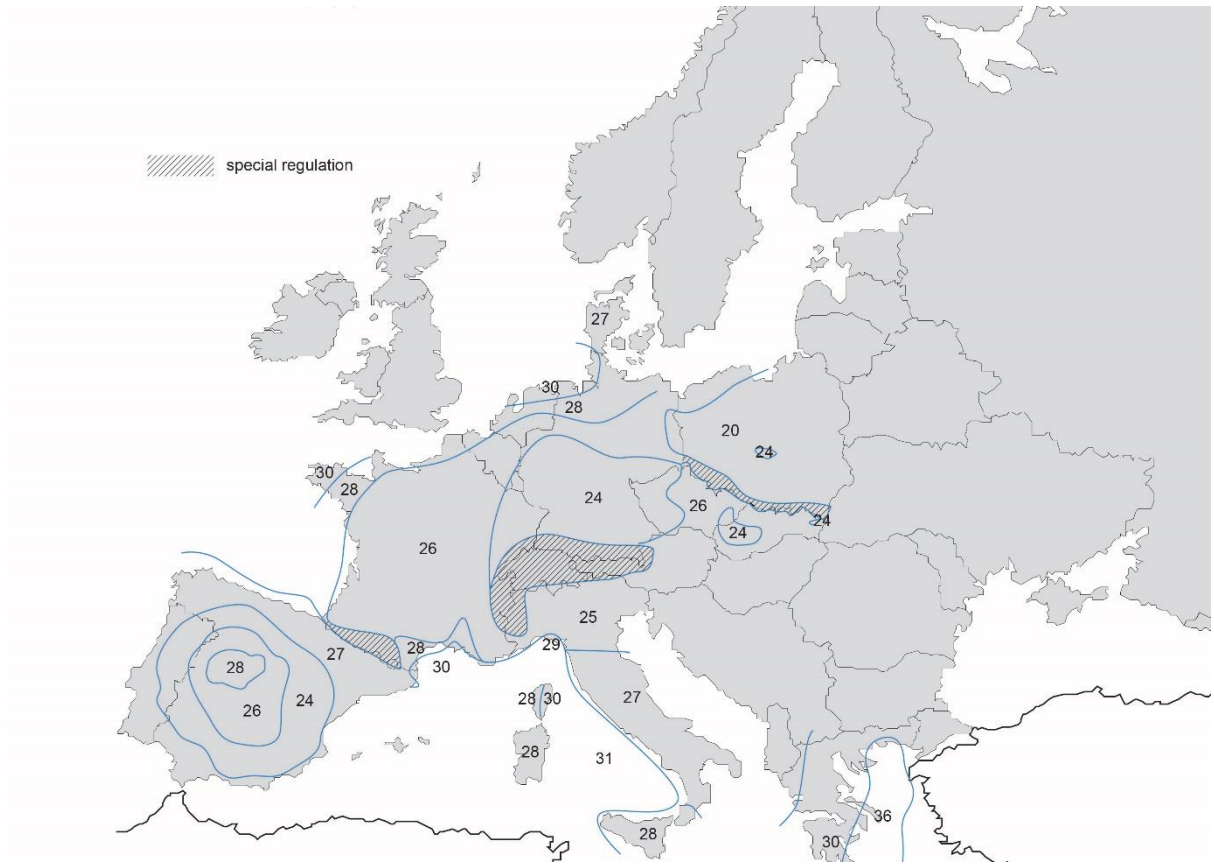


Fig. 1: Central and Mediterranean Europe wind map (map source [19])

2 Design approach

This paper aims to introduce a digital architectural design method based on the reciprocal interaction of architecture and the wind. The building form, global, as well as local, plays a fundamental role concerning wind-induced actions. The geometric features of the building, and, in the case of flexible building skins, the mechanical properties (aero-elastic effects) of such skin alter the wind load and the wind pattern around the buildings [5]. The ultimate wind effect on structures is, naturally, influenced by the approaching wind characteristics.

2.1 Wind-adaptive envelope

The wind on building envelopes acts as surface pressure; positive is compression, while

negative is suction. Depending on the direction and strength of the wind, buildings and their structures are subjected to variable pressure. This paper proposes a wind-adaptive building envelope that passively responds to the instant wind pressure in real-time. The geometry and material-based adaptive behavior consequently can contribute to the optimal utilization of the designed structure in various load conditions [20]. As contrary to the conventional inert structures which have to resist the external energy caused by the wind, adaptive structures can be designed as more lightweight because of their ability to comply with the external forces, transforming the wind energy into kinetic energy. The access kinetic energy could be used to generate electricity. The adaptive behavior can be particularly useful in case of unpredictable, swiftly altering events, such as wind storms.

2.2 Tensegrity-membrane adaptive element

The wind-adaptive envelope is developed digitally using the afore-mentioned software ergo Rhinoceros and Grasshopper. Translucency, as well as lightness, is the main criteria for the proposed adaptive skin. A tensegrity (tensional integrity) [21] structural configuration is employed to create the tensegrity-membrane adaptive module. The following reasons led to this choice: lightness, flexibility under the load (reversible passive deformation caused by the material-embedded properties), and structural stability ensured by the force equilibrium of tensioned and compressed elements. The principle of the shape adaptation of the adaptive module is depicted in Figure 2. The extent of the module's bending depends on the material properties, the direction of the acting wind, as well as the wind speed. The whole wind-adaptive envelope comprises of multiple adaptive modules, each fixed in 4 points to the supporting structural frame. One adaptive module consists of struts in compression, steel cables in tension, and two layers of translucent tensile fabric membranes in tension. A live physics engine Kangaroo 2, an add-on for Grasshopper, is used for finding the equilibrium state of the proposed tensegrity-membrane configuration. Depending on the speed of the acting wind, represented by the pressure, the adaptive module creating the adaptive envelope, bends and rotates adequately.

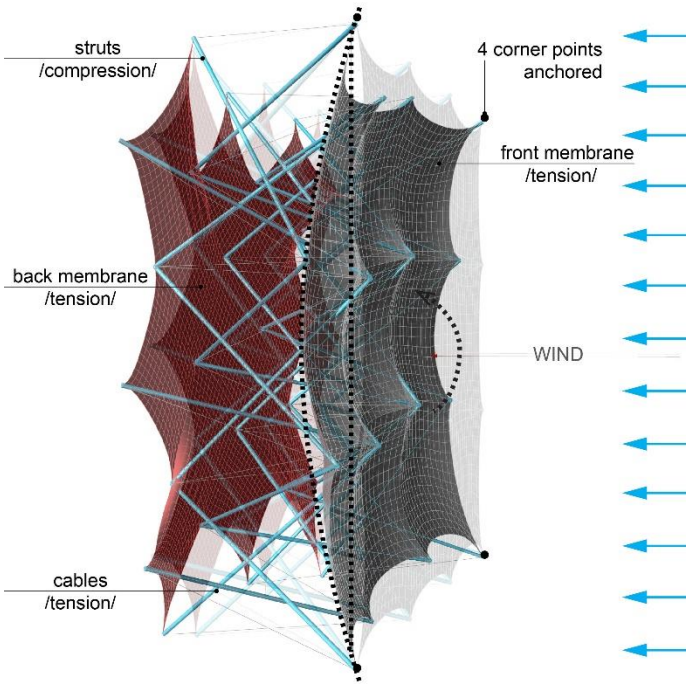


Fig. 2: One tensegrity-membrane module of the adaptive envelope (dotted is the bending and rotation under certain wind pressure)

Table 1 describes the material properties defined in the Kangaroo 2 simulation for examining the reconfiguration of the proposed adaptive element under the wind load.

Table 1. Material settings.

	Length *l* [m]	**Diameter *Φ* *or* thickness *h* [m]**	**Stiffness *k* [N/m]**	**Young's Modulus *E* [Pa]**	**Pretension 0=max.; 1=min. [-]**
Struts	1	$\Phi = 16e^{-3}$	2 110 080	$10.5e^{9}$	1
Cables	0.78	$\Phi = 2e^{-3}$	523 333	$130e^{9}$	0.99
Membranes (isotropic)	2.1 x 2.1	$h = 0.51e^{-3}$	20 000 or 84 000	$3.9\ e^{7}$ or $16.5e^{7}$	0.90

2.3 Wind analysis of buildings of basic geometric shapes

CFD tests of basic-geometry building shapes are conducted to compare the influence of the wind-adaptive (morphing in the wind) building envelope versus the non-adaptive (steady) variant on the building aerodynamics. Swift, a plug-in for Grasshopper, running on the OpenFOAM® platform, is used to perform the simulations. The post-processing of the simulations' results is possible using stand-alone software, Paraview. The results are captured in the 2D top and side view. The finite volume method meshing is used to divide the virtual wind tunnel to 1x1x1 m cells. Closer to the tested geometry, the cells are refined to 0.125 x

0.125 x 0.125 m. The terrain roughness is set to 1, representing densely built-up areas. The convergence criteria are the following: velocity *U*, pressure *p*, turbulent model *k/ε*: $1e^{-2}$, $4e^{-2}$, $1e^{-2}$, respectively. It is suitable to set the relaxation factors for p = 0.3 and U, k, ε = 0.7 to achieve faster convergence. The pressure used in Swift is the kinematic pressure p_k [16]:

$$p_k = \frac{p}{\rho} \#(1)$$

where p_k is the kinematic pressure used for incompressible flows [m^2/s^2], p is the static pressure [Pa], and ρ is the air density [kg/m^3].

The basic-shape objects will also be examined for their resistance to the wind flow, represented by the drag force, F_d:

$$F_d = -\frac{1}{2c_d A \rho v^2} \# (2)$$

where F_d is the drag force [N], c_d is the drag coefficient [-], ρ is the air density [kg/m^3], v is the wind speed [m/s].

3 Design experimentation

Creating an adaptive architecture able to react simultaneously with the changing wind conditions, requires a sequential analysis from the local (morphed) shape to the global building form, assessing their behavior in the wind. First, the live physics simulations have to be employed to obtain the shape change caused by the acting wind. Second, the changed geometry configuration is tested in Swift CFD plug-in.

3.1 Digital simulations for creating a wind-adaptive shape-changing module

Nine 4-strut tensegrities create one shape-changing module, which is fixed in 4 corner points of the front membrane and morphs when loaded by the wind pressure (Fig. 2). The adaptive modules can be arrayed on any surface, covering or substituting building envelopes. This study deals with the latter. Two size versions of the adaptive module are examined in the paper, i.e., 2.1 x 2.1 m, and 4 x 4 m. The wind-responding envelope in two size variants is applied as a skin on each building surface, only on the windward side, or fully covering the building. The dimensions of the tested cube are 12x12x12 m, the cylinder is 12 m high, and 12 m in diameter. The interactive shape response of the whole building shape in the wind is achieved using Kangaroo 2 (Fig. 4), alike the simulation of one element. The bending in the wind, however, is simplified, as only the material characteristics of the front membrane are defined in the simulation, representing the building surface in contact with the wind flow. By changing the wind speed, the particle-spring system in Kangaroo 2 reconfigures to find another equilibrium state. Consequentially, the wind force acting on such an adaptive building envelope creates a dimpled, rough surface (Fig. 5). The value of the wind pressure in Pa is derived from Bernoulli's equation:

$$p = \frac{1}{2}\rho v^2 \#(3)$$

where p is the wind pressure [Pa], ρ is the density of air [kg/m^3], and v is the wind velocity [m/s]. Hence, in Kangaroo 2 simulations, the wind speed of 24 m/s is represented by the pressure of 360 Pa, acting on the windward side of buildings.

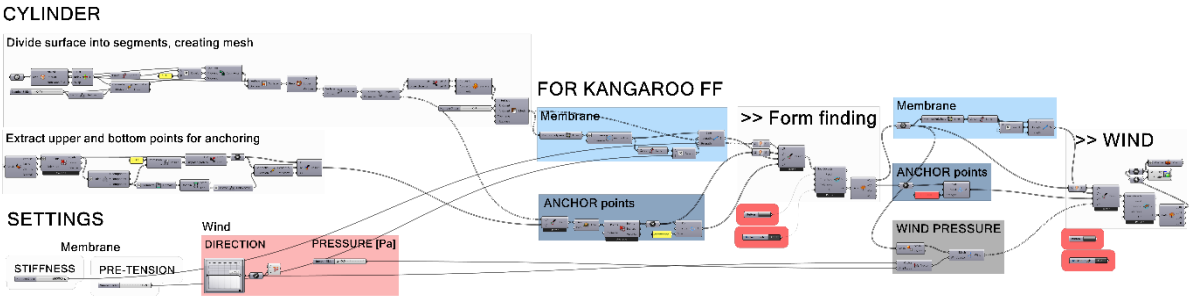


Fig. 4: The Grasshopper definition, employing Kangaroo 2. The membrane material properties, as well as the magnitude of the wind, influence the shape change

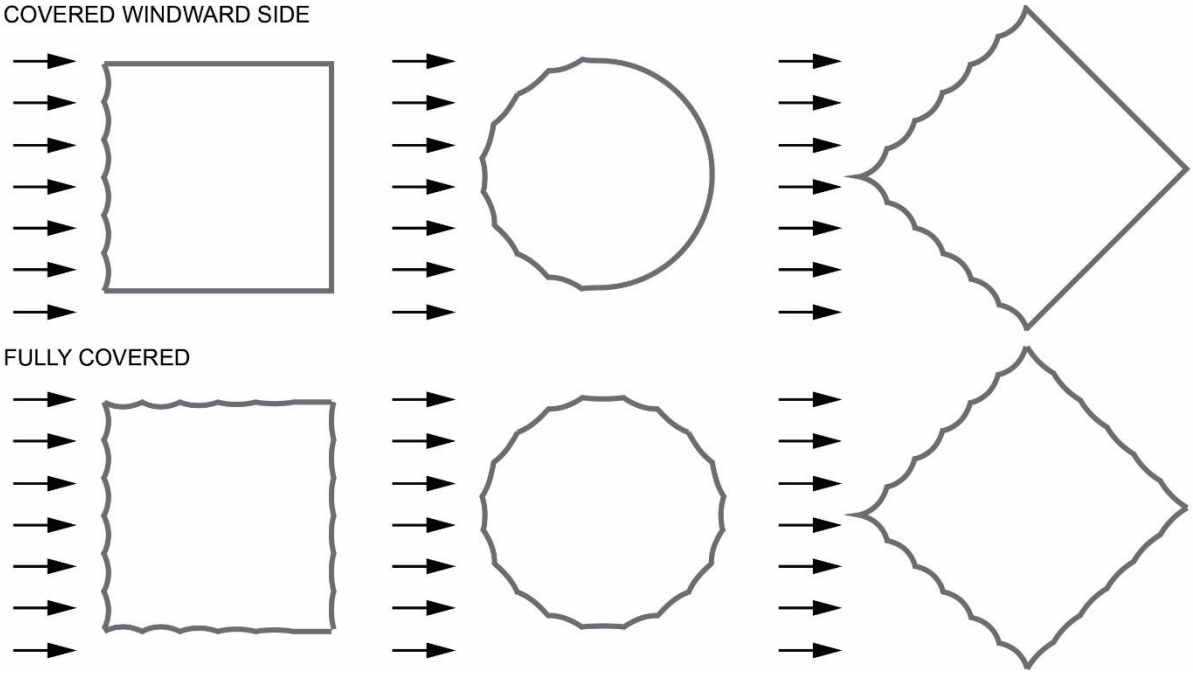


Fig. 5: The top view of the cube, cylinder, and 45-degrees rotated cube with the wind-deformed skin

3.2 CFD simulations

After the wind-induced shape response of the adaptive envelope is found, the CFD analysis follows. Experiments with basic shapes (Fig. 6, 7, and 8) in the 24 m/s wind are performed to examine the surface wind pressure and drag force reduction, as well as the influence on the wind flow pattern. Three simulation cases are run for all three tested shapes. First, a smooth-surface building is tested, second, a shape with 2x2 m adaptive modules (fully or partially covering the object) is analyzed, and third, a variant with a 4x4 m adaptive module (fully or partially covering the object) is simulated using the CFD solver, Swift. Subsequently, the visualizations, as well as the calculations of the surface pressure p_k, as well as the drag force

F_d, representing the resistance of the tested object to the wind flow, are performed using Paraview.

4 Results

The smooth variant is compared with four variants of adaptive façade for each basic shape. The results for the surface kinematic pressure p_k as well as for the shape's drag force F_d are described in Table 2.

Table 2. Numerical results of the CFD simulations.

Basic shape	**maximum Negative pressure p_k on the building surface** [m^2/s^2]	**Maximum Positive pressure p_k on the building surface** [m^2/s^2]	**Drag force F_d** [N]
Smooth cube	**-375.37**	**+302.41**	**-44 088**
Cube with 2x2m dimples (windward adaptive façade)	-378.28 (↑ 0.8%)	+303.20	-44 614 (↑ 1.2%)
Cube with 2x2m dimples (whole façade is adaptive)	-917.57 (↑↑ 144%)	+303	-41 289 (↓ 6.3%)
Cube with 4x4m dimples (windward adaptive façade)	-368.49 (↓ 1.8%)	+303.91	-45 351 (↑ 2.9%)
Cube with 4x4m dimples (whole façade is adaptive)	-1075.74 (↑↑ 187%)	+301.66	-39 950 (↓ 9.4%)
Smooth cylinder	**-748.23**	**+296.36**	**-16 317**
Cylinder with 2x2m dimples (windward adaptive façade)	-886.34 (↑ 18.5%)	+295.99	-15 217 (↓ 6.7%)
Cylinder with 2x2m dimples (whole façade is adaptive)	-815.41 (↑ 8.9%)	+295.81	-14 979 (↓ 8.2%)
Cylinder with 4x4m dimples (windward adaptive façade)	-1015.87 (↑ 35.8%)	+295.82	-17 770 (↑ 8.9%)
Cylinder with 4x4m dimples (whole façade is adaptive)	-1005.24 (↑ 34.3%)	+296.43	-21 362 (↑ 31%)
Smooth 45° cube	**-908.75**	**+294.24**	**-57 785**

45° Cube with 2x2m dimples (windward adaptive façade)	-1182.39 (↑ 30.1%)	+298.20	-57 666 (↓ 0.2%)
45° Cube with 2x2m dimples (whole façade is adaptive)	-937.69 (↑ 3.2%)	+299.42	-41 373 (↓ 28.4%)
45° Cube with 4x4m dimples (windward adaptive façade)	-1033.61 (↑ 13.7%)	+299.00	-60 130 (↑ 4.3%)
45° Cube with 4x4m dimples (whole façade is adaptive)	-1011.76 (↑ 11.3%)	+299.25	-43 341 (↓ 25%)

4.1 Numerical extremities

The actual values of the wind pressure, as well as drag force, are obtained in Paraview post-processing software. Although the results indicate that the suction is not reduced when the adaptive skin is applied, when every finite volume calculation cell was examined, it was observed, that there are some calculation extremities on the tested geometries. These extremities are caused by the spiky shape of the adaptive surface, combined with the size of the finite volume calculation cell. After the extremities are obviated, this can alter the actual values of the wind suction. This issue will be addressed in further research.

4.2 The cube

The wind flow separation is induced on the front edges of the object, causing the fluid flow to change into turbulence. The smooth cube produces symmetrical swirls on the sides of the geometry, while the speed can reach 20 m/s. Downwind, the speed is around 15 m/s. The wind suction is visible on the sides, more to the back of the geometry.

After applying the wind-adaptive envelope on the front side of the cube, similar symmetrical swirls develop downwind, however, the speed is reduced to circa 12 m/s. The wind suction zones on the sides move closer to the front side of the geometry.
The adaptive surface with larger dimples (4x4 m), applied on the front side of the cube, behaves similarly as the 2x2 m variant. The symmetrical swirls on the leeward side develop closer to the geometry, while new areas of downwind suction are formed. In addition to the observations of the wind flow, the actual values of surface pressure, as well as drag force, are examined. In 24 m/s winds, the applied adaptive skin with the 2x2 m dimples does not contribute to reducing the surface wind suction. Nevertheless, the wind suction is slightly reduced when the 4x4 m variant is employed. The drag force increases after applying the adaptive envelope, due to the discernible spikes, caused by high wind speed.

The 2x2 m adaptive envelope covering the whole surface of the cube contributes to the reduction of the suction zones around the object, and the wind swirls on the sides of the cube. The extreme increase of the surface wind pressure acting on the object could be caused by the numerical extremities. The 4x4 m variant contributes to decreasing the drag force on the object. On the leeward side, a longer calm zone is formed, and the wind swirls on

the sides of the cube are eliminated. The wind pressure around the object is diffused, influencing the reduction of the wind suction zones. The reduced pressure zones around the cube suggest that the actual values of the surface wind pressure are probably influenced by the numerical extremities and consequently will be much lower.

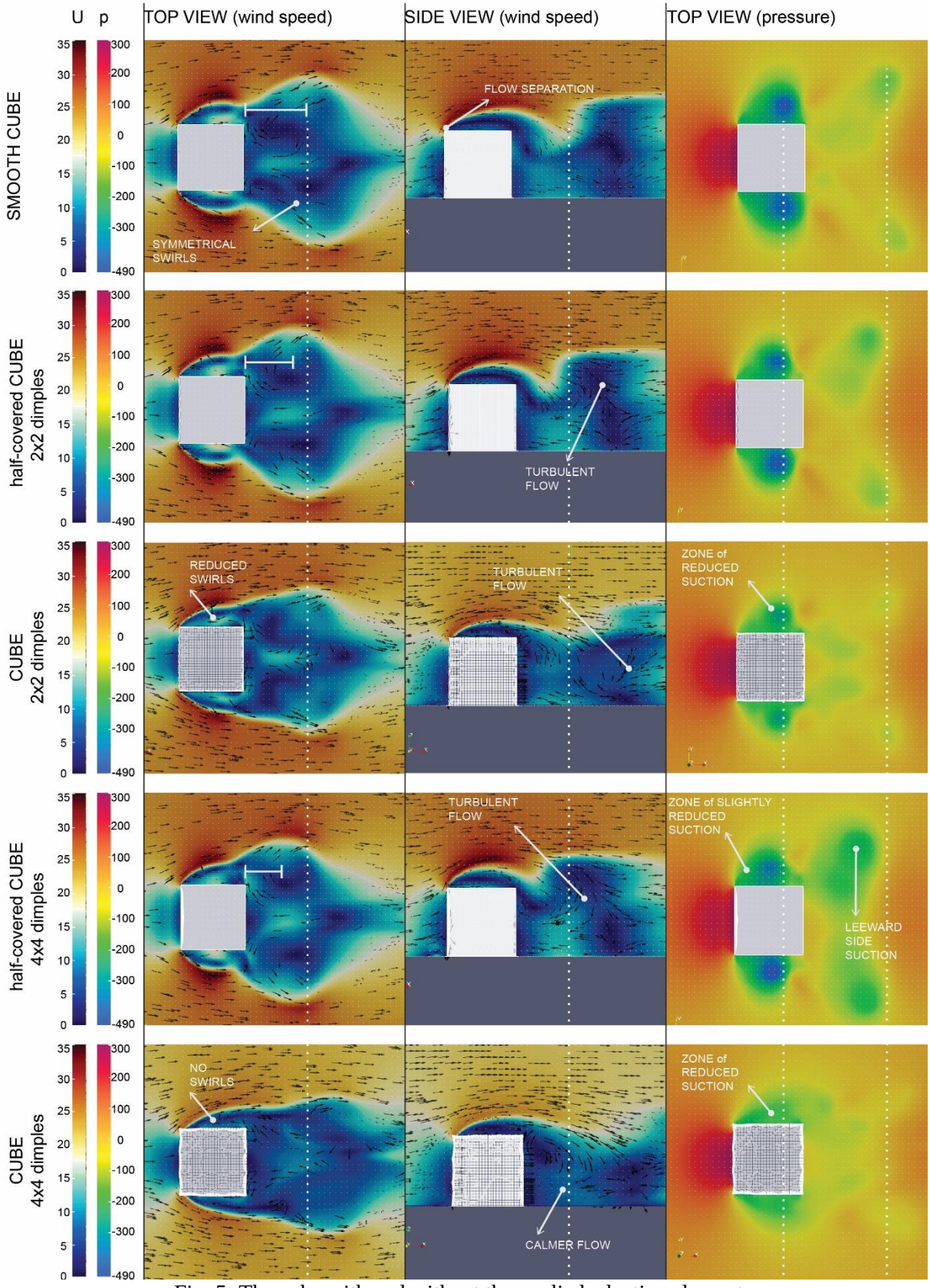


Fig. 5: The cube with and without the applied adaptive elements

4.3 The cylinder

The cylinder geometry with a smooth surface causes the wind to grow very turbulent in the downwind zone with high wind speeds, reaching 10-25 m/s. The cylinder, as an obstacle to the wind, does not provide a sheltered zone from the wind. The wind flow separates very early, which causes a strong suction after the flow separation, as well as high wind speeds on the sides of the geometry.

The cylinder half-covered in the 2x2 m dimples can slightly reduce the surface wind suction on the object. The separation of the wind flow moves towards the windward side of the cylinder, which consequently straightens the flow downwind, creating a wind-sheltered zone behind the object. The drag force is decreased by 6.7%. The 4x4 m windward side-variant induces the formation of downwind suction zones. The wind swirls with the speed of 5-20 m/s form on the leeward side of the object.

After the adaptive envelope with the dimensions of one adaptive element of 2x2 meters is applied on the whole surface of the cylinder, the influence on the wind flow pattern is very distinct. Although symmetrical wind swirls form on the leeward side, the wind speed is reduced to 0-5 m/s, rising again in the center of the swirl. The zone of wind suction on the sides is reduced. The drag force is decreased by 8.2%. After the application of 4x4 m dimples on the whole surface of the cylinder, the wind flow is straightened downwind. The zone of the strong suction (around -400 m2/s2), is further reduced.

Even though the surface suction and the drag force rise after the application of the dimpled adaptive envelope, the wind flow is undoubtedly calmer downwind.

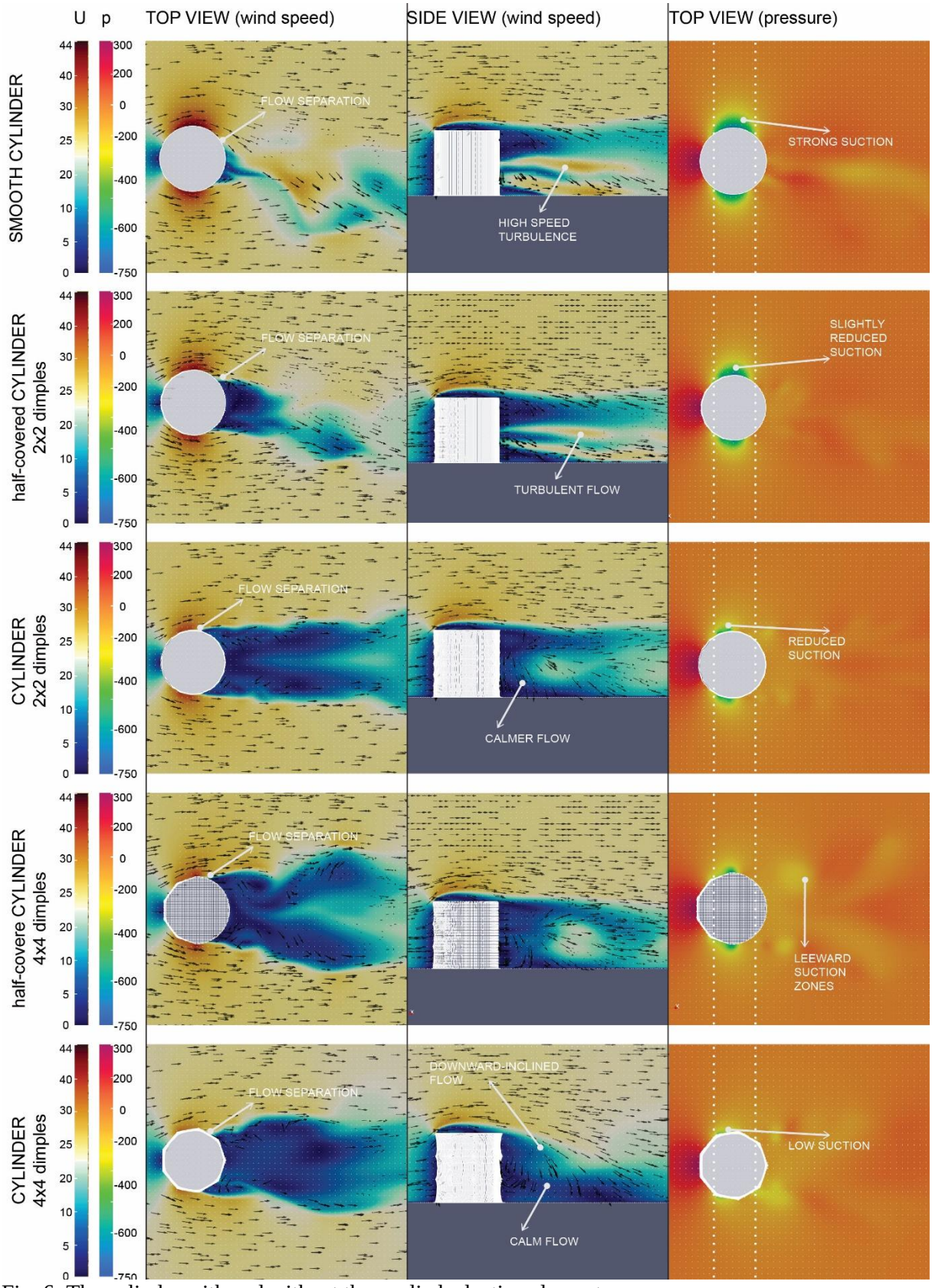


Fig. 6: The cylinder with and without the applied adaptive elements

4.4 The cube rotated 45° towards the flow

The wind flow is due to the edgy geometry of the cube, separated on the side edges. The long downwind zone, with symmetrical swirls, is induced by the smooth-surface variant.

The cube with the 2x2 m dimpled surface, applied on the side of the wind approach, contributes to reducing the wind speed to 0-10 m/s. The wind suction on the leeward side is diffused and slightly reduced. The application of the adaptive envelope on the whole surface of the cube surprisingly causes a significant, 28.4% decrease of the drag force. The high-speed wind is downward-inclined early downwind. The width of the leeward-side wind-covered zone is reduced. Leeward side high-pressure zones form closer to the tested object.

With the 4x4 m dimples applied on the windward side, the symmetrical wind swirls are slightly calmer. The drag force increases with the more distinct spikes caused by the wind, acting on the adaptive envelope. The adaptive envelope fully covering the 45-degrees-rotated cube causes the wind flow to incline downward quite early downwind. The wind-shielded zone is narrow, compared to the half-covered variant. The 25% decrease of drag force can be achieved when the dimpled surface covers the whole cube, in spite of the spiky geometry.

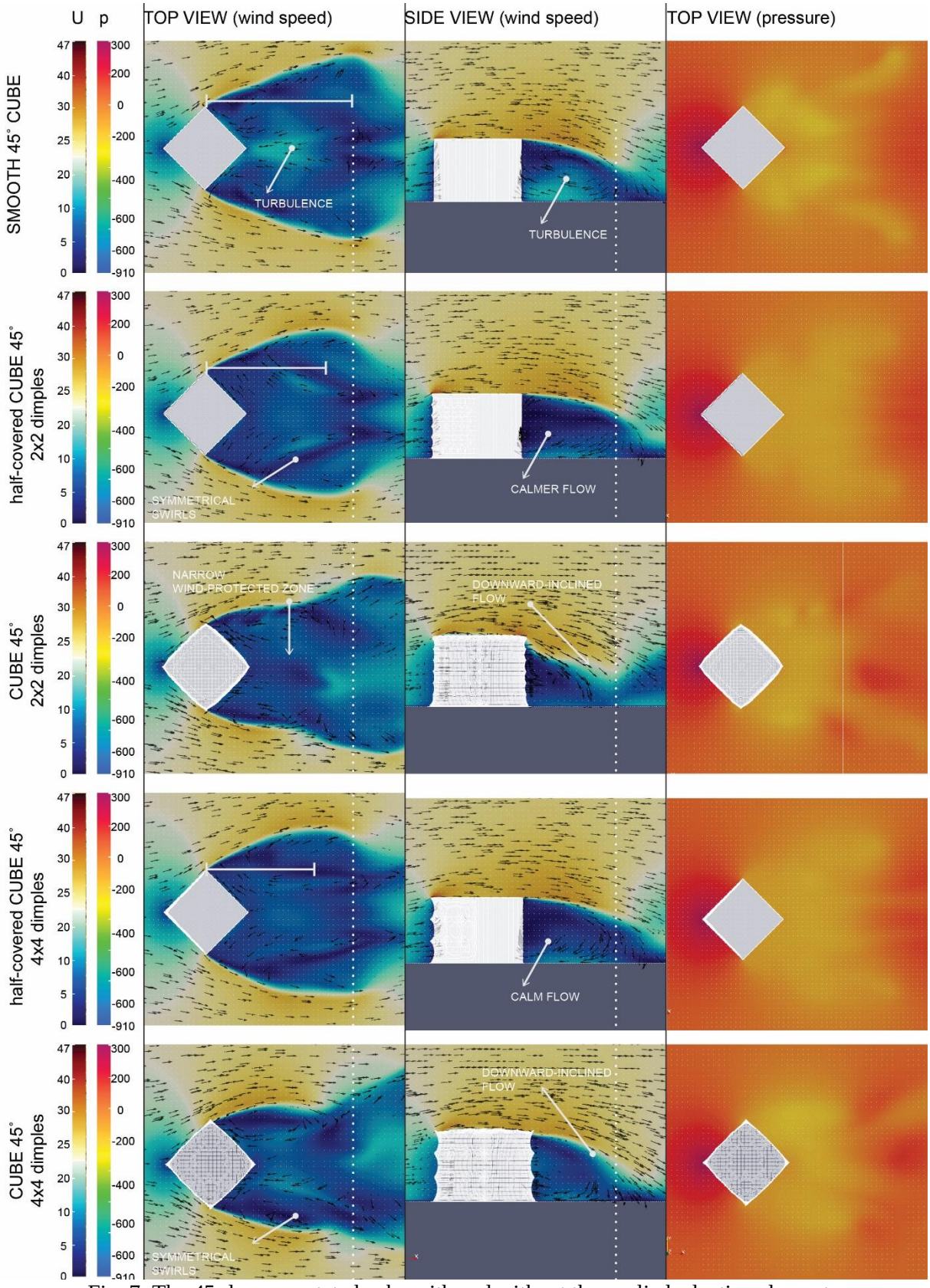


Fig. 7: The 45-degrees rotated cube with and without the applied adaptive elements

5 Conclusion

As was demonstrated by this research, the wind, through the local passive shape change of building envelopes, influences the flow pattern and suction zones around buildings, as well as the drag force and surface wind pressure. The designed adaptive module, exposed to the wind force, bends under this load, creating a dimpled building surface. The bending is directly dependent on the wind pressure magnitude and is reversible due to the tensegrity-membrane geometry. The simulations of the lightweight wind-adaptive building envelope in high, 24 m/s wind speed were performed for three building shape variants. Smooth building envelopes, as well as buildings fully covered or half-covered in adaptive envelopes, were reciprocally compared. Two sizes of adaptive modules were tested, and the results were evaluated from two aspects: the building's surface wind pressure and drag force reduction, as well as the character of the wind pressure and the wind flow pattern around the tested shapes.
The results show that the global shape of the building influences the ultimate effect the adaptive skin has on the wind. A reduction of drag force of 6.3% and 9.4% compared to the smooth variant can be achieved when a 2x2 m and 4x4 m (respectively) adaptive envelope covers the whole cube-shaped building. Juxtaposed to the smooth-surface cylinder, a 6.7% reduction of drag force can be achieved on a cylindrically-shaped building, half-covered with a 2x2 m adaptive envelope. The drag force can be decreased by 8.2% when the 2x2 m adaptive envelope fully covers the cylinder. A notable reduction of the drag force is observed when the 45-degrees rotated cube is fully covered in a 2x2 m adaptive envelope (28.4% reduction), as well as for the 4x4 m variant (25% reduction). Despite the decrease of the surface wind suction is not confirmed, it is assumed, that the extreme increase can be the result of the calculation extremities. This issue will be addressed in further research. The observations of the wind flow pattern confirm that the designed wind-adaptive envelope can have a strong influence on the downwind zone and create an area; shadowed from the wind (this is valid for all tested shapes).

Acknowledgements

This research was funded by the Grant Agency of the Slovak Republic. The project numbers are VEGA 1/0674/18 and VEGA 1/0129/20.

References

[1] J. P. den Hartog, A. Koutamanis, and P. G. Luscuere, "Possibilities and limitations of CFD simulation for indoor climate analysis," in *Fifth Design and Decision Support Systems in Architecture and Urban Planning - Part one: Architecture Proceedings*, 2000, pp. 152–167.

[2] J.-Y. Tsou, "Applying computational fluid dynamics to architectural design development," in *Proceedings of The Third Conference on Computer Aided Architectural Design Research in Asia*, 1998, pp. 133–142.

[3] F. Moukalled, L. Mangani, and M. Darwish, *Fluid Mechanics and Its Applications*, vol. 113. Springer, 2016.

[4] D. H. J. Chung and L. C. Malone-lee, "Computational Fluid Dynamics for urban design," in *New Frontiers: Proceedings of the 15th International Confer- ence on Computer-Aided Architectural Design Research in Asia CAADRIA 2010*, 2010, pp. 357–366.

[5] A. Giacchetti, G. Bartoli, and C. Mannini, "Wind Effects on Permeable Tall Building Envelopes: Issues and Potentialities," *CTBUH Journal*, pp. 20–27, 2019.
[6] T. J. Scanlon, "A NUMERICAL ANALYSIS OF FLOW AND DISPERSION AROUND A CUBE Thomas," *A Numer. Anal. FLOW Dispers. AROUND A CUBE Thomas*, no. 1977, 1991.
[7] C. Yuan *et al.*, "Multilayer urban canopy modelling and mapping for traffic pollutant dispersion at high density urban areas," *Sci. Total Environ.*, vol. 647, pp. 255–267, Jan. 2019.
[8] S. Sanquer, G. Caniot, and S. Bandhare, "Wind assessment in urban area with cfd tools application to natural ventilation potential and outdoor pedestrian comfort," *14th Int. Conf. IBPSA - Build. Simul. 2015, BS 2015, Conf. Proc.*, pp. 1684–1691, 2015.
[9] L. Lignarolo, C. Lelieveld, and P. Teuffel, "Shape morphing wind-responsive facade systems realized with smart materials," in *Proceedings of the Adaptive Architecture Conference*, 2011, no. March, pp. 1–14.
[10] L. Kabošová, "The search for an optimal architectural shape using wind performance analysis," *IOP Conf. Ser. Mater. Sci. Eng.*, vol. 566, no. 1, pp. 1–5, 2019.
[11] K. Kuismanen, "Climate-conscious architecture: Design and wind testing method for climates in change," University of Oulu, 2008.
[12] W. Janssen, B. Blocken, and T. Van Hooff, "Use of Cfd Simulations to Improve the Pedestrian Wind Comfort Around a High-Rise Building in a Complex Urban Area," in *13th Conference of International Building Performance Simulation Association, Chambéry, France, August 26-28*, 2013, pp. 1918–1925.
[13] R. A. M. Castro, "Wind analysis in the early design stage : An empirical study of wind visualisation techniques for architects," 2015.
[14] A. Chronis, A. Dubor, E. Cabay, and M. S. Roudsari, "Integration of CFD in computational design: An evaluation of the current state of the art," in *Proceedings of the 35th International Conference eCAADe: ShoCK! Sharing of Computable Knowledge!*, 2017, pp. 601–610.
[15] S. Stankovic and A. Setrakian, "Air Flow Modelling - 1."
[16] R. A. Moya Castro, D. Prohasky, S. Watkins, Y. Ding, J. Burry, and M. Burry, "Aerodynamic strategy applied in an urban shelter design - Simulation and analysis of aerodynamic phenomena in an urban context," *eCAADe 2014 Fusion - data Integr. its best*, vol. 1, pp. 137–144, 2014.
[17] I. Olekšáková, O. Hubová, and L. Konečná, "Influence of nearby structure on the wind flow around the cube structure," *Rocz. Inz. Bud.*, vol. 15, pp. 29–36, 2015.
[18] Eurocode 1, *Actions on structures, Part 1-4: general actions. Wind actions*. Brussels, 2010.
[19] S. O. Hansen, "Wind loading design codes," in *Fifty years of wind engineering: Prestige lectures from the sixth European and African conferece on wind engineering*, 2012, pp. 35–68.
[20] G. Senatore, P. Duffour, and P. Winslow, "Energy and Cost Assessment of Adaptive Structures: Case Studies," *J. Struct. Eng. (United States)*, vol. 144, no. 8, pp. 1–23, 2018.
[21] R. Motro, *Tensegrity: Structural Systems for the Future*, 1st ed. Butterworth-Heinemann, 2003.